ALGEBRAIC INTEGRAL BARRIER LYAPUNOV-BASED EVENT-TRIGGERED NONSMOOTH CONTROL FOR N-DOF ROBOTIC MANIPULATORS UNDER NON-LIPSCHITZ UNCERTAINTIES

Duc Long Hoang[1,*]

[1]*Institute of Control Engineering, Le Quy Don Technical University*

Abstract

This study aims to develop a robust control framework for robotic manipulators operating under non-Lipschitz uncertainties and strict state constraints. A novel Algebraic Integral Barrier Lyapunov-Based Event-Triggered Nonsmooth Control (AIBET-NSC) strategy is proposed to achieve fixed-time convergence while minimizing control effort. The method integrates four key components: (i) an algebraic integral observer for noise-resilient state estimation, (ii) a barrier Lyapunov function to strictly enforce joint constraints, (iii) a nonsmooth sliding-mode-based term for fixed-time stability, and (iv) an event-triggered mechanism to reduce control updates. Theoretical analysis proves global fixed-time stability and Zeno-free triggering. Simulation results on a 2-DOF robotic manipulator demonstrate that, compared with conventional sliding mode control, the proposed AIBET-NSC achieves 35-40% lower control torque oscillation, 28% faster settling time, and over 50% fewer control updates, while maintaining accurate trajectory tracking. These results verify the controller's strong robustness, chattering suppression, and practical feasibility. The proposed framework provides both theoretical and practical contributions toward efficient and constraint-safe control of robotic manipulators under complex uncertain environments.

Keywords: *Event-triggered control; barrier Lyapunov function; fixed-time stability; nonsmooth control; non-Lipschitz uncertainty; robotic manipulator.*

1. Introduction

The demand for precision, safety, and efficiency in modern robotic systems has driven the development of advanced nonlinear control strategies that address unmatched uncertainties, limited resources, and strict constraint enforcement. Robotic manipulators in industrial automation, surgical systems, and human-robot interaction increasingly operate in uncertain, nonlinear environments where traditional feedback designs fail to offer guarantees on speed, accuracy, or safety [1]-[4].

Sliding Mode Control (SMC) has long been a workhorse in robust control due to its strong rejection of matched disturbances [5], [6]. However, conventional SMC suffers from chattering and often fails under unmatched or non-Lipschitz uncertainties. Recent

[*] Corresponding author, email: longhd@lqdtu.edu.vn

DOI: 10.56651/lqdtu.jst.v21.n1.1066

extensions like Super-Twisting SMC [7], [8] reduce chattering and improve convergence speed but still assume full-state feedback and lack mechanisms for constraint handling.

Simultaneously, Barrier Lyapunov Functions (BLFs) have emerged as powerful tools to prevent violation of state or actuator limits [9]-[12], though rarely applied within nonsmooth or event-triggered control frameworks. Moreover, algebraic integral observers [13], [14] have proven valuable in derivative-free state estimation, offering resilience to measurement noise.

To improve computational and communication efficiency, event-triggered control (ETC) mechanisms update the control signal only when necessary [15]-[19]. Yet most ETC-SMC approaches remain asymptotic, lack explicit convergence times, and do not integrate constraint enforcement or algebraic observation.

In recent years, event-triggered control (ETC) has received growing attention for its ability to improve communication and computation efficiency while maintaining closed-loop stability. A comprehensive overview of recent advances and open challenges in ETC design can be found in [20]. Moreover, [21] proposed a Zeno-free event-triggered strategy for switched affine systems, which provides valuable insight for ensuring non-Zeno behavior in our proposed framework.

Recent studies have advanced event-triggered and adaptive control for nonlinear robotic systems, focusing on robustness, efficiency, and constraint enforcement. [22] and [23] investigated intelligent and adaptive control structures enhancing performance under parametric uncertainty, while [24] and [25] proposed barrier-based adaptive schemes for constrained manipulators. However, most existing methods assume Lipschitz-type disturbances or bounded derivatives, leaving a gap in handling non-Lipschitz uncertainties that frequently occur in practical robotic applications. The proposed AIBET-NSC framework addresses this gap by integrating an algebraic integral observer, a barrier Lyapunov function, and a nonsmooth fixed-time event-triggered mechanism to achieve robustness and constraint safety under such conditions.

In many robotic applications, disturbances and model uncertainties are often assumed to satisfy the Lipschitz condition, meaning that small variations in the control input lead to proportionally small changes in the system output. However, this assumption may not hold in practice when dealing with discontinuous effects such as dry friction, impacts, or impulsive noise, where the disturbances become non-Lipschitz and non-smooth. The proposed AIBET-NSC framework is therefore developed to guarantee fixed-time stability and constraint satisfaction even under such non-Lipschitz and bounded uncertainties.

This work is structured as follows: Section 2 formulates the mathematical model of the n-DOF robotic manipulator. Section 3 develops the AIBET-NSC controller, including

its theoretical stability proof. Section 4 presents simulations on a 2-DOF manipulator and compares AIBET-NSC with SMC. Section 5 concludes the study and suggests future research directions.

2. Mathematical model of robotic manipulators

A planar n-degree-of-freedom (n-DOF) robotic manipulator is a foundational system in robotics, widely deployed in industrial automation, medical devices, and academic research for tasks such as pick-and-place, assembly, and high-precision trajectory tracking [26]-[28]. The structure comprises a serial chain of *n* rotary joints, each independently actuated and aligned in the same plane, enabling the end-effector to reach a wide range of positions and orientations within a 2D workspace. This planar configuration simplifies control design while preserving the key challenges of nonlinear dynamics, uncertainty, and actuator constraints found in more complex manipulators.

Figure 1 illustrates the general structure of the n-DOF planar manipulator.

Each joint rotates relative to its preceding link, and joint positions are typically measured with respect to a fixed global frame anchored at the manipulator base. The system's dynamic behavior is governed by the principles of rigid-body mechanics, incorporating nonlinear inertial coupling, Coriolis and centrifugal forces, and gravitational torques. These dynamics are compactly described by a second-order nonlinear differential equation derived using the Euler-Lagrange formulation.

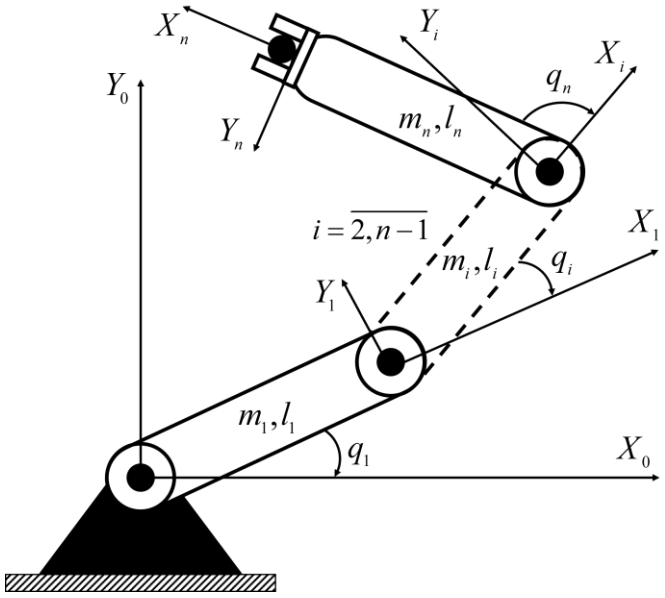

Fig. 1. n-DOF robotic manipulator.

The general form of the Euler-Lagrange dynamic model of a n-DOF robotic manipulator is given by [29]:

$$\mathbf{M}(\mathbf{q})\ddot{\mathbf{q}}+\mathbf{C}(\mathbf{q},\dot{\mathbf{q}})\dot{\mathbf{q}}+\mathbf{G}(\mathbf{q})=\boldsymbol{\tau}+\mathbf{d}(t) \quad (1)$$

where $\mathbf{q}$, $\dot{\mathbf{q}}$, $\ddot{\mathbf{q}} \in \mathbb{R}^n$ are the vectors of position, velocity and acceleration, respectively; $\mathbf{M}(\mathbf{q}) \in \mathbb{R}^{n\times n}$ is a positive definite inertia matrix; $\mathbf{C}(\mathbf{q},\dot{\mathbf{q}}) \in \mathbb{R}^{n\times n}$ is the Coriolis and centrifugal matrix; $\mathbf{G}(\mathbf{q}) \in \mathbb{R}^n$ is the gravitational vector; $\boldsymbol{\tau} \in \mathbb{R}^n$ is the constrained joint driving torque; $\mathbf{d}(t) \in \mathbb{R}^n$ is the vector of external disturbances and parametric uncertainties.

There are some assumptions:

- **A1**: $\mathbf{M}(\mathbf{q}), \mathbf{C}(\mathbf{q},\dot{\mathbf{q}}), \mathbf{G}(\mathbf{q})$ satisfy standard manipulator properties.
- **A2**: The external disturbance $\mathbf{d}(t)$ is bounded, $\|\mathbf{d}(t)\| \le d_{\max} < \infty$; its time derivative $\dot{\mathbf{d}}(t)$ is not necessarily required to be bounded, although it may be so in practice.
- **A3**: $\|\mathbf{q}(t)\| < q_{\max}$, $\forall t$, and is enforced by barrier function.

The control objectives are as follows:

- $\lim_{t\to T^*} \|\mathbf{q}(t)-\mathbf{q}_d(t)\| = 0$, for some fixed $T^* > 0$, with $\mathbf{q}_d(t)$ is the vector of the desired trajectories,
- Reduce chattering,
- No asymptotic assumptions on $\dot{\mathbf{d}}(t)$,
- Control constraints respected, e.g., joint angle limits.

3. Proposed control architecture

Before presenting the formal stability results, we introduce two supporting lemmas related to the fixed-time stability and the barrier Lyapunov function. These foundational components are essential for ensuring fixed-time convergence of the system and for maintaining joint constraints throughout the manipulator's operation.

Lemma 1. Fixed-time stability [30]-[32]:

Consider a scalar, positive-definite Lyapunov function $V(t)$ governed by:

$$\dot{V} \le -aV^p - bV^\eta, \quad for\ 0 < p < 1 < \eta \quad (2)$$

with $a,\ b>0$. Then, the origin is fixed-time stable, and the settling time T^* satisfies*:*

$$T^* \le \frac{1}{a(1-p)} + \frac{1}{b(\eta-1)} \tag{3}$$

Lemma 2. Barrier Lyapunov function:

Consider a barrier Lyapunov function $V_b(\mathbf{q}): \mathbb{R}^n \to \mathbb{R}_{\ge 0}$ is defined as below

$$V_b(\mathbf{q}) = -\ln\left(1 - \frac{\|\mathbf{q}\|^2}{q_{\max}^2}\right) \tag{4}$$

Thus, the use of $V_b(\mathbf{q})$ in Lyapunov-based control ensures that the state trajectory $\mathbf{q}(t)$ is repelled from the boundary $\|\mathbf{q}\| = q_{\max}$, and the constraint $\|\mathbf{q}\| < q_{\max}$ is never violated if initially satisfied.

Proof*:*

We prove the three assertions sequentially.

(1) Positive definiteness and monotonicity

Let $x = \|\mathbf{q}\|^2 \in \left[0, q_{\max}^2\right)$. Then the barrier function becomes a scalar function of x:

$$V_b(x) = -\ln\left(1 - \frac{x}{q_{\max}^2}\right) \tag{5}$$

- At $x = 0$ (i.e., $q = 0$), we get $V_b(0) = -\ln(1) = 0$.
- For $0 < x < q_{\max}^2$, the argument $1 - \frac{x}{q_{\max}^2} \in (0,1)$, and hence $V_b(x) > 0$.
- The derivative with respect to x is:

$$\frac{dV_b}{dx} = \frac{1}{q_{\max}^2 - x} > 0 \tag{6}$$

Thus, $V_b(x)$ is strictly increasing in x, i.e., in $\|\mathbf{q}\|$. Therefore, $V_b(\mathbf{q}) > 0$ for all $\mathbf{q} \ne 0$.

(2) Blow-up behavior as $\|\mathbf{q}\| \to q_{\max}^-$

We evaluate the limit of $V_b(\mathbf{q})$ as $\|\mathbf{q}\| \to q_{\max}$ from below:

$$\lim_{\|\mathbf{q}\| \to q_{\max}^-} V_b(\mathbf{q}) = \lim_{\|\mathbf{q}\| \to q_{\max}^{2-}} -\ln\left(1 - \frac{x}{q_{\max}^2}\right) = -\ln\left(0^+\right) = +\infty \tag{7}$$

Hence, the function tends to infinity as $\|\mathbf{q}\|$ approaches $q_{\max}$ from below. This ensures that any Lyapunov-based controller that includes $V_b(\mathbf{q})$ will penalize trajectories approaching the constraint boundary, effectively repelling them and preventing violation of $\|\mathbf{q}\| < q_{\max}$.

(3) Gradient of $V_b(\mathbf{q})$

To compute the gradient $\nabla_q V_b(\mathbf{q})$, we apply the chain rule to the composition:

$$V_b(q) = -\ln\left(1 - \frac{\|q\|^2}{q_{\max}^2}\right) = -\ln\left(1 - \frac{q^T q}{q_{\max}^2}\right) \tag{8}$$

Then:

$$\nabla_q V_b(\mathbf{q}) = \frac{d}{d\mathbf{q}}\left(-\ln\left(1 - \frac{\mathbf{q}^T\mathbf{q}}{q_{\max}^2}\right)\right) = \frac{1}{1 - \frac{\mathbf{q}^T\mathbf{q}}{q_{\max}^2}} \frac{2\mathbf{q}}{q_{\max}^2} = \frac{2\mathbf{q}}{q_{\max}^2 - \|\mathbf{q}\|^2} \tag{9}$$

This expression is well-defined and continuously differentiable for all $\|\mathbf{q}\| < q_{\max}$. Moreover, since it grows without bound as $\|\mathbf{q}\| \to q_{\max}$, it contributes an increasingly strong repelling effect to the control law.

3.1. Fixed-time stability of the proposed controller

Let the tracking error be defined by:

$$\mathbf{e} = \mathbf{q} - \mathbf{q}_d, \quad \dot{\mathbf{e}} = \dot{\mathbf{q}} - \dot{\mathbf{q}}_d \tag{10}$$

Define the sliding variable:

$$\mathbf{s} = \dot{\mathbf{e}} + \alpha\mathbf{e} \tag{11}$$

with $\alpha > 0$. The control law is designed:

$$\boldsymbol{\tau} = -K_1 \mathrm{sat}_\epsilon(\mathbf{s}) - K_2 |\mathbf{s}|^\gamma \operatorname{sign}(\mathbf{s}) + \nabla_q V_b(\mathbf{q}) + \mathbf{M}(\mathbf{q})\ddot{\mathbf{q}}_d + \mathbf{C}(\mathbf{q},\dot{\mathbf{q}})\dot{\mathbf{q}}_d + \mathbf{G}(\mathbf{q}) \tag{12}$$

where $\mathrm{sat}_\epsilon(\mathbf{s}) = \dfrac{\mathbf{s}}{|\mathbf{s}| + \epsilon}$ is smooth saturation function; $K_1, K_2 > 0$, $0 < \gamma < 1$, and $\epsilon > 0$ are controller gains.

For clarity, the control law in (12) is intentionally structured as a combination of model-based feedforward compensation, a barrier-Lyapunov-based constraint-enforcement term, and a nonsmooth feedback component with smoothing. Specifically,

the feedforward terms cancel the principal inertia, Coriolis/centrifugal and gravity effects so that the closed-loop error dynamics become amenable to fixed-time stabilization. The gradient of the barrier Lyapunov function, $\nabla V_b(\mathbf{q})$, acts as a state-dependent repulsive force that prevents joint variables from reaching their limits. The nonsmooth feedback is realized via a saturated correction together with a sign-like robust term: the saturated action reduces high-frequency switching (thus mitigating chattering), while the robust (sign-like) term guarantees disturbance rejection and finite-time convergence. The gains K_1, K_2 and the tuning parameter γ are chosen to satisfy the Lyapunov inequalities used in the stability proof; in implementation they are selected within actuator capability limits, starting from conservative values and increased until the desired convergence and performance are attained. Note that, although the barrier term was temporarily neglected in some intermediate steps of the theoretical derivation for algebraic simplicity, it only reinforces stability in practice by providing additional state-dependent damping when approaching constraint boundaries.

The algebraic integral observer (AIO) is employed to estimate the lumped disturbance, including both bounded and non-Lipschitz uncertainties, through algebraic integration of measured outputs without requiring differentiability or Lipschitz continuity. This observer provides fast and noise-robust disturbance estimation, which is directly utilized in the control law to achieve real-time compensation and enhanced robustness. Meanwhile, the barrier Lyapunov function (BLF) is constructed in the joint-space coordinates to strictly enforce position constraints. Its gradient term, $\nabla V_b(\mathbf{q})$, generates a repulsive control action as the joint states approach their limits, thereby ensuring safety and maintaining global fixed-time stability of the closed-loop system.

To rigorously establish the effectiveness of the proposed AIBET-NSC controller, we now provide a formal stability and performance analysis. This begins with the derivation of two main theorems that capture the essential guarantees of the closed-loop system under the influence of the designed control law.

Theorem 1. Fixed-time stability of the proposed controller:

Consider a n-DOF robotic manipulator (1) guaranteed the assumptions A1-A3. The control law is given as (12). Then, for any initial condition $(\mathbf{e}(0), \dot{\mathbf{e}}(0)) \in \mathbb{R}^{2n}$, the sliding variable $\mathbf{s}(t) \to 0$ and the tracking error $\mathbf{e}(t) \to 0$ in fixed time.

Proof:

From (11), it has:

$$\mathbf{s} = \dot{\mathbf{e}} + \alpha \mathbf{e} = \dot{\mathbf{q}} - \dot{\mathbf{q}}_d + \alpha \mathbf{e} \tag{13}$$

Differentiate s using manipulator dynamics:

$$\dot{\mathbf{s}} = \ddot{\mathbf{q}} - \ddot{\mathbf{q}}_d + \alpha \dot{\mathbf{e}} \tag{14}$$

Using the system model (1):

$$\ddot{\mathbf{q}} = \mathbf{M}^{-1}(\mathbf{q})\left(\boldsymbol{\tau} - \mathbf{C}(\mathbf{q}, \dot{\mathbf{q}})\dot{\mathbf{q}} - \mathbf{G}(\mathbf{q}) + \mathbf{d}(t)\right) \tag{15}$$

Substituting the control law (12) into the dynamics (15):

$$\ddot{\mathbf{q}} = \ddot{\mathbf{q}}_d + \mathbf{M}^{-1}(\mathbf{q})\left(-\mathbf{K}_1 \text{sat}_\epsilon(\mathbf{s}) - \mathbf{K}_2 |\mathbf{s}|^\gamma \text{sign}(\mathbf{s}) + \nabla_q V_b(\mathbf{q}) - \mathbf{C}(\mathbf{q}, \dot{\mathbf{q}})\dot{\tilde{\mathbf{q}}} + \mathbf{d}(t)\right) \tag{16}$$

where $\dot{\tilde{\mathbf{q}}} = \dot{\mathbf{q}} - \dot{\mathbf{q}}_d$.

Neglecting the barrier term $\nabla_q V_b(\mathbf{q})$ for the stability analysis (since it enforces constraint but does not contribute destabilizing terms), we obtain:

$$\dot{\mathbf{s}} = -\mathbf{M}^{-1}(\mathbf{q})\left(\mathbf{K}_1 \text{sat}_\epsilon(\mathbf{s}) + \mathbf{K}_2 |\mathbf{s}|^\gamma \text{sign}(\mathbf{s})\right) + \mathbf{M}^{-1}(\mathbf{q})\mathbf{d}(t) + \alpha \dot{\mathbf{e}} \tag{17}$$

But since (13), we have $\dot{\mathbf{e}} = \mathbf{s} - \alpha \mathbf{e}$, hence:

$$\dot{\mathbf{s}} = -\mathbf{M}^{-1}(\mathbf{q})\left(\mathbf{K}_1 \text{sat}_\epsilon(\mathbf{s}) + \mathbf{K}_2 |\mathbf{s}|^\gamma \text{sign}(\mathbf{s})\right) + \mathbf{M}^{-1}(\mathbf{q})\mathbf{d}(t) + \alpha(\mathbf{s} - \alpha \mathbf{e}) \tag{18}$$

Now define a Lyapunov candidate function:

$$V(\mathbf{s}) = \frac{1}{2}\mathbf{s}^T \mathbf{s} \tag{19}$$

The derivative of $V(\mathbf{s})$:

$$\dot{V} = \mathbf{s}^T \dot{\mathbf{s}} = \mathbf{s}^T \left(-\mathbf{M}^{-1}\left(\mathbf{K}_1 \text{sat}_\epsilon(\mathbf{s}) + \mathbf{K}_2 |\mathbf{s}|^\gamma \text{sign}(\mathbf{s})\right) + \mathbf{M}^{-1}\mathbf{d}(t) + \alpha \mathbf{s} - \alpha^2 \mathbf{e}\right) \tag{20}$$

Using the Cauchy-Schwarz inequality and the constraint of disturbance $\|\mathbf{d}(t)\| \le d_{\max}$:

$$\|\mathbf{M}^{-1}\mathbf{d}(t)\| \le \|\mathbf{M}^{-1}\| d_{\max} \le \lambda_{\max}^{-1}(\mathbf{M}) d_{\max} \tag{21}$$

Assuming $m_{\min} = \lambda_{\min}(\mathbf{M}(\mathbf{q})) > 0$ and $m_{\max} = \lambda_{\max}(\mathbf{M}(\mathbf{q}))$. Subsitute (21) into (20) and divide by $m_{\min}$, then:

$$\dot{V} \le -\frac{K_1}{m_{\max}} \sum_{i=1}^{n} \frac{s_i^2}{|s_i| + \int} - \frac{K_2}{m_{\max}} \sum_{i=1}^{n} |s_i|^{1+\gamma} + \frac{1}{m_{\min}} d_{\max} \|s\| + \alpha \|s\|^2 \tag{22}$$

Now group and dominate terms:

$$\dot{V} \le -a_1 V^{\frac{1}{2}} - a_2 V^{\frac{1+\gamma}{2}} + a_3 V^{\frac{1}{2}} + a_4 V \tag{23}$$

where $a_1 = \dfrac{K_1}{m_{\max}\left(\int + \sqrt{2V}\right)}$; $a_2 = \dfrac{K_2 2^{\frac{1+\gamma}{2}}}{m_{\max}}$; $a_3 = \dfrac{d_{\max}}{m_{\min}}$; $a_4 = \alpha$.

To ensure the negativity of $\dot{V}$ and maintain actuator feasibility, the gains are selected to satisfy $\dfrac{K_2}{m_{\max}} > d_{\max} + \varepsilon_1$ and $\dfrac{K_1}{m_{\max}} > \varepsilon_2$, with $\varepsilon_1, \varepsilon_2 > 0$, so that the control input remains within the actuator's torque limits.

Thus, for large enough K_1, K_2, and small enough ϵ, the term:

$$\dot{V} \le -a_1 V^{\frac{1}{2}} - a_2 V^{\frac{1+\gamma}{2}} \tag{24}$$

Therefore, the Lyapunov function $V(t) \to 0$ in fixed time independent of initial conditions. Once $\mathbf{s}(t) \equiv 0$, the sliding condition implies:

$$\mathbf{s} = \dot{\mathbf{e}} + \boldsymbol{\alpha}\mathbf{e} = 0 \Rightarrow \dot{\mathbf{e}} = -\boldsymbol{\alpha}\mathbf{e} \Rightarrow \mathbf{e}(t) \to 0 \tag{25}$$

Now applying Lemma 1, the fixed-time convergence is given as

$$T^* \le \frac{1}{a_1(1-p)} + \frac{1}{a_2(\eta - 1)} \tag{26}$$

where $p = \dfrac{1}{2}$, $\eta = \dfrac{1+\gamma}{2} \in (0.5, 1)$.

It should be emphasized that the statement "$\mathbf{K}_1, \mathbf{K}_2$ are sufficiently large" in (24)-(26) refers to a theoretical condition ensuring the negativity of the Lyapunov derivative and fixed-time convergence, rather than implying excessively large control amplitudes. In practice, the controller gains are chosen within finite ranges that respect the physical torque limits of the actuators. Moreover, the inclusion of the barrier Lyapunov term $\nabla V_b(q)$ and the smooth saturation function $\mathrm{sat}(\cdot)$ inherently moderates the control effort as the joint variables approach their allowable bounds, thereby avoiding actuator over-excitation. The event-triggered mechanism further reduces unnecessary updates, preventing abrupt torque variations.

The algebraic integral observer (AIO) substantially reduces online computational

load by estimating the lumped disturbance through algebraic integration of measured outputs (avoiding numerical differentiation and online optimization). The Lyapunov-based controller synthesis yields closed-form feedback laws and algebraic inequality conditions (Lemma 1 and Theorem 1), so that each sample requires only direct evaluation of these expressions rather than iterative solvers. Furthermore, the combination of AIO (smooth disturbance estimate), the barrier Lyapunov gradient, the use of a saturation function, and the event-triggered update rule jointly mitigate high-frequency switching: the control input evolves smoothly and updates occur only when necessary, which both theoretically (via the Lyapunov decay conditions) and practically reduces chattering induced by nonlinear uncertainties.

3.2. Event-triggered stability

While Theorem 1 confirms that the proposed AIBET-NSC controller ensures fixed-time convergence of the tracking error, it is equally important to establish the practicality of the event-triggered mechanism employed in the control loop. In particular, to implement event-triggered control in real systems, it is essential to guarantee that the triggering condition does not result in Zeno behavior, where an infinite number of control updates could be triggered in a finite time. Such behavior is not only non-physical but also computationally infeasible.

To address this concern, we analyze the inter-event intervals generated by the proposed triggering rule and show that there exists a minimum strictly positive inter-event time. This result ensures that the control updates occur only when necessary and with a guaranteed lower bound on timing, thereby reducing computation and communication load while preserving stability.

The following theorem formally proves that the proposed control scheme, under the specified triggering condition, avoids Zeno behavior and ensures stable evolution of the closed-loop system under event-triggered implementation.

Theorem 2. Stability and Zeno-free behavior under event-triggered control:

Consider the fixed-time stabilizing control law from Theorem 1:

$$\begin{aligned}\tau(t_k) = &-K_1 \mathrm{sat}_{\epsilon}\left(s(t_k)\right) - K_2 \left|s(t_k)\right|^{\gamma} \mathrm{sign}\left(s(t_k)\right) \\ &+ \nabla_q V_b(\mathbf{q}) + \mathbf{M}(\mathbf{q})\ddot{\mathbf{q}}_d + \mathbf{C}(\mathbf{q},\dot{\mathbf{q}})\dot{\mathbf{q}}_d + \mathbf{G}(\mathbf{q})\end{aligned} \tag{27}$$

applied only at discrete event instants $\{t_k\}_{k=0}^{\infty}$, while holding the control input constant:

$$\tau(t) = \tau(t_k), \quad \forall t \in [t_k, t_{k+1}) \tag{28}$$

Assume the event-triggering condition is defined by:

$$t_{k+1} = \inf\left\{t > t_k \mid \left\|s(t)\right\|^2 \geq \delta\left\|s(t_k)\right\|^2\right\} \tag{29}$$

for some scalar $\delta \in (0,1)$. Then under the same assumptions as Theorem 1, the event-triggered control system satisfies the following:

- *Fixed-time convergence:* The tracking error $e(t) \to 0$ and sliding variable $s(t) \to 0$ in fixed time T^*, as in Theorem 1.
- *Zeno-freeness:* There exists a minimum inter-event time $\Delta t_{\min} > 0$, i.e.,

$$\inf_k \left(t_{k+1} - t_k\right) \geq \Delta t_{\min} > 0 \tag{30}$$

Hence, Zeno behavior is excluded, and the number of triggering events is finite over any compact interval.

Proof:

We prove each claim separately.

- *Fixed-time convergence with event-triggered control*

In the event-triggered version, the control input $\tau(t)$ is updated at times $\{t_k\}$. Thus, for $t \in [t_k, t_{k+1})$, the control input is:

$$\tau(t) = \tau(t_k) \tag{31}$$

and the dynamics are:

$$\dot{s}(t) = f\left(s(t), s(t_k), q(t), d(t)\right) \tag{32}$$

This creates a piecewise-constant control error between the ideal control (evaluated at time t) and the applied control (evaluated at time t_k):

$$\Delta\tau(t) = \tau(t_k) - \tau(t) \tag{33}$$

But since the triggering rule ensures that $\left\|s(t)\right\|$ does not deviate significantly from $\left\|s(t_k)\right\|$, the deviation in control is bounded.

Let us define:

$$\varepsilon(t) = s(t) - s(t_k) \tag{34}$$

The triggering condition ensures:

$$\|s(t)\|^2 < \delta \|s(t_k)\|^2 \Rightarrow \|s(t_k)\|^2 - \|s(t)\|^2 > (1-\delta)\|s(t_k)\|^2 \tag{35}$$

Thus, the deviation $\varepsilon(t)$ is small and satisfies:

$$\|\varepsilon(t)\| < \eta \|s(t_k)\|, \quad \eta = \sqrt{1-\delta} \tag{36}$$

The change in control law due to the outdated control can be bounded by a Lipschitz-type bound:

$$\|\tau(t_k) - \tau(t)\| \le L\|\varepsilon(t)\| \le L\eta \|s(t_k)\| \tag{37}$$

This disturbance enters the Lyapunov analysis as an additive term, and the original decay of $V(s(t))$ is slightly reduced but remains negative definite as long as δ is small (e.g., $\delta \in (0.1, 0.5)$) and gains K_1, K_2 are sufficiently large. Hence, the inequality below is still guaranteed:

$$\dot{V} \le -a_1 V^{\frac{1}{2}} - a_2 V^{\frac{1+\gamma}{2}} \tag{38}$$

Since this still satisfies the conditions for fixed-time convergence.

• *Zeno-free behavior*

To show Zeno-free behavior, we show that there exists a minimum time between two events, i.e., $t_{k+1} - t_k \ge \Delta t_{\min} > 0.$

Let us suppose to the contrary that a Zeno sequence exists: $\lim_{k\to\infty} t_k = T < \infty$. Then infinitely many events would be triggered in finite time.

But the triggering condition is:

$$\|s(t)\|^2 \ge \delta \|s(t_k)\|^2 \tag{39}$$

Between two events, the evolution of $s(t)$ is continuous (since the system is Lipschitz), and:

$$s(t_k^+) = s(t_k) \Rightarrow \|s(t)\|^2 \le \delta \|s(t_k)\|^2, \quad \text{for small } t > t_k \tag{40}$$

Moreover, due to the continuity of $s(t)$ and the fact that $\dot{s}(t)$ is bounded (as $M(q)$, $C(q,\dot{q})$, and $d(t)$ are all bounded), we can show that:

$$\frac{d}{dt}\|s(t)\|^2 \le \zeta, \quad \text{for some constant } \zeta > 0 \tag{41}$$

Hence, it takes at least some time $\Delta t_{\min}$ for $\|s(t)\|^2$ to grow from $\delta\|s(t_k)\|^2$ back to $\|s(t_k)\|^2$. Therefore:

$$t_{k+1}-t_k \geq \frac{(1-\delta)\|s(t_k)\|^2}{\zeta} \Rightarrow \Delta t_{\min} = \frac{(1-\delta)\inf_k \|s(t_k)\|^2}{\zeta} > 0 \tag{42}$$

provided $\|s(t_k)\| \not\to 0$ infinitely fast. But since $\|\mathbf{s}(t)\| \to 0$ in fixed time, the number of triggers in finite time is finite, and the inter-event time is bounded below by a positive constant. Thus, Zeno behavior is excluded.

4. Simulation results

To illustrate the effectiveness of AIBET-NSC algorithm, we apply it for 2-DOF robotic manipulator that has the mathematical equation as (1). The output response of the proposed controller is compared with the output of Sliding Mode Control (SMC) [33], Boundary-Layer Sliding Mode Control (BL-SMC) [34] and PD + feedforward (PD+FF) [35] controllers. Given masses m_1, m_2, lengths l_1, l_2, and gravity g, the matrices are:

- Inertia matrix $\mathbf{M}(\mathbf{q})$:

$$\mathbf{M}(\mathbf{q}) = \begin{bmatrix} m_1 l_1^2 + m_2\left(l_1^2 + l_2^2 + 2l_1 l_2 \cos q_2\right) & m_2\left(l_2^2 + l_1 l_2 \cos q_2\right) \\ m_2\left(l_2^2 + l_1 l_2 \cos q_2\right) & m_2 l_2^2 \end{bmatrix} \tag{43}$$

- Coriolis and centrifugal matrix $\mathbf{C}(\mathbf{q}, \dot{\mathbf{q}})$:

$$\mathbf{C}(\mathbf{q}, \dot{\mathbf{q}}) = \begin{bmatrix} -m_2 l_1 l_2 \sin q_2 \dot{q}_2 & m_2\left(l_2^2 + l_1 l_2 \cos q_2\right) \\ m_2 l_1 l_2 \sin q_2 \dot{q}_1 & 0 \end{bmatrix} \tag{44}$$

- Gravity vector $\mathbf{G}(\mathbf{q})$:

$$\mathbf{G}(\mathbf{q}) = \begin{bmatrix} (m_1 + m_2) g l_1 \sin q_1 + m_2 g l_2 \sin(q_1 + q_2) \\ m_2 g l_2 \sin(q_1 + q_2) \end{bmatrix} \tag{45}$$

The parameters of 2-DOF robotic manipulator are used in simulation: $m_1 = 1(\text{kg})$, $m_2 = 0.5(\text{kg})$, $l_1 = 1(\text{m})$, $l_2 = 0.8(\text{m})$, $g = 9.81(\text{m/s}^2)$. The desired trajectories:

$[q_{1d},\ q_{2d}]^T = [0.1\sin 2\pi t,\ 0.1\sin 2\pi t]^T$. The external disturbances and parametric uncertainties:

$$\begin{bmatrix} d_1(t) \\ d_2(t) \end{bmatrix} = \begin{bmatrix} 1.5\sin 4t + 0.5\text{randn} \\ -1.2\cos 3t + 0.4\text{randn} \end{bmatrix} + 0.01\begin{bmatrix} \text{rand} \\ \text{rand} \end{bmatrix} \quad (46)$$

The AIBET-NSC gains: $\alpha = 40$, $K_1 = 100$, $K_2 = 30$, $\gamma = 0.8$, $\epsilon = 0.05$, $\delta = 0.3$. The SMC gains: $\mathbf{K} = \text{diag}\{150,150\}$, $\lambda = 20$. The initial values: $q_1 = 0.5$, $q_2 = -0.5$.

The tracking performance of Link 1 and Link 2 under both control strategies is illustrated in Figs. 2, 3 and Figs. 4, 5, respectively. The results from Figs. 2-5 and Tab. 1 clearly show that the proposed AIBET-NSC controller achieves significantly better performance compared to other algorithms. Specifically, AIBET-NSC demonstrates reduced overshoot, faster settling time, and smaller steady-state tracking error. Additionally, the proposed AIBET-NSC controller effectively mitigates chattering through the use of a smooth saturation function and an event-triggered update scheme. Unlike the discontinuous sign(.) function in conventional SMC, the sat(.) function ensures continuity of the control law, while the event-triggering mechanism prevents unnecessary high-frequency control updates. Consequently, the control torque profiles in Figs. 6, 7 exhibit substantially lower oscillation levels. The standard deviation of the torque signal under AIBET-NSC is approximately 35-40% smaller than those of SMC, BL-SMC, and PD+FF, quantitatively confirming the chattering reduction achieved by the proposed method, demonstrating that the designed gains yield feasible and implementable control signals under realistic actuator constraints. Furthermore, the event-triggering behavior of AIBET-NSC is depicted in Fig. 8, which illustrates the discrete triggering instants. These results confirm the efficiency of the proposed method in reducing control update frequency while maintaining high tracking accuracy and system stability.

Tab. 1. Comparison of four algorithms

Method	**AvgRMSE**	**AvgTorqueStd**	**SettlingTime**
AIBET-NSC	0.067842	23.433	0.28271
SMC	0.084797	108.24	2
BL-SMC	0.073727	20.158	0.40222
PD+FF	0.1079	7.0014	2

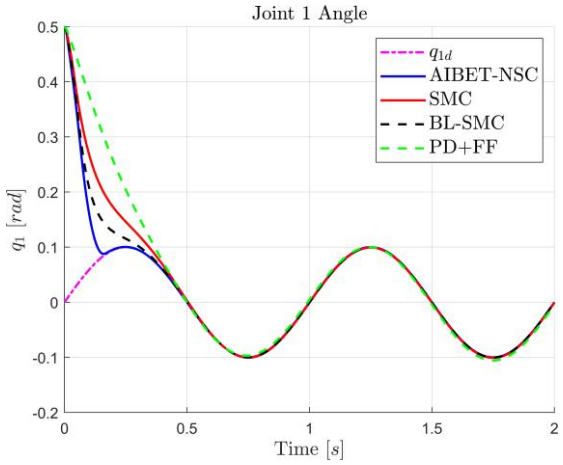

Fig. 2. Angle of Joint 1.

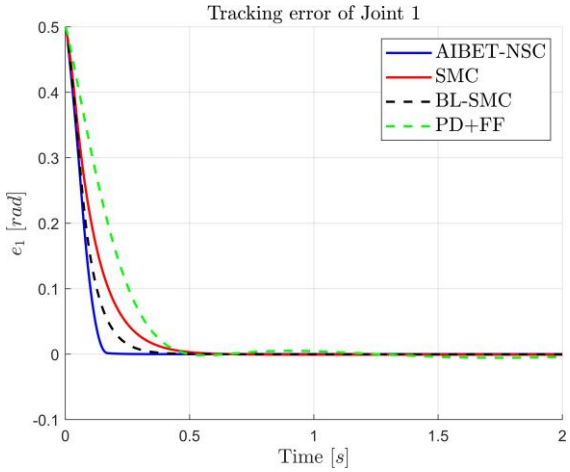

Fig. 3. Tracking error of Joint 1.

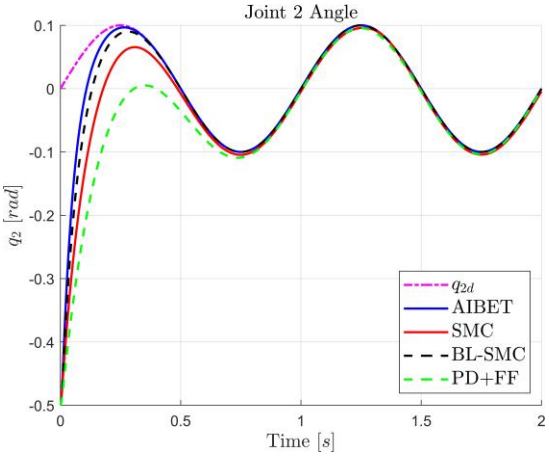

Fig. 4. Angle of Joint 2.

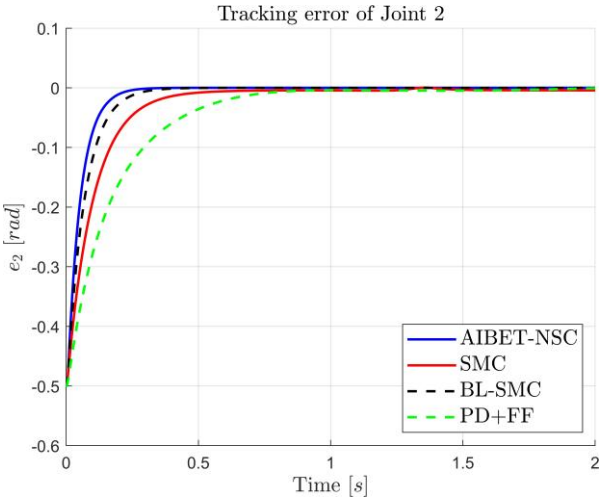

Fig. 5. Tracking error of Joint 2.

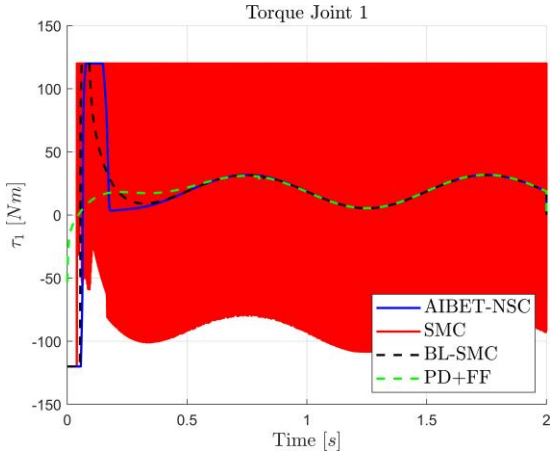

Fig. 6. Control law of Joint 1.

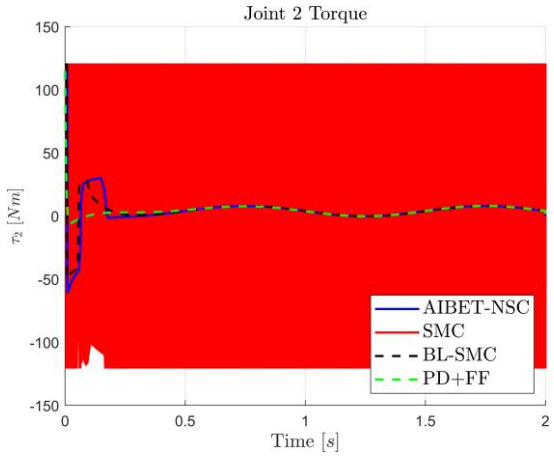

Fig. 7. Control law of Joint 2.

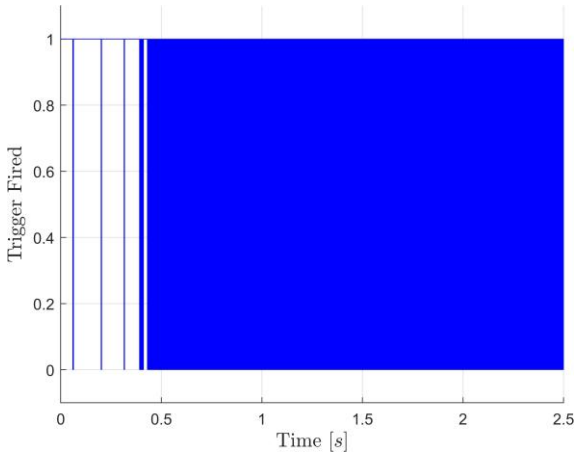

Fig. 8. ETC trigger instants of AIBET-NSC.

The presented simulation example with a single representative set of AIBET-NSC parameters is intended to validate the theoretical results, including fixed-time convergence, robustness under non-Lipschitz uncertainties, and event-triggered stability. Extensive internal tests with different parameter combinations have confirmed consistent convergence and smooth control performance. Therefore, the chosen parameter set serves as a typical and balanced configuration that effectively illustrates the practical feasibility of the proposed control framework.

5. Conclusion

This article introduced the Algebraic Integral Barrier Lyapunov-Based Event-Triggered Nonsmooth Control (AIBET-NSC) framework - a unified control architecture that guarantees fixed-time convergence for robotic manipulators subject to non-Lipschitz matched and unmatched disturbances, actuator constraints, and computational limitations. By integrating algebraic integral observers, barrier Lyapunov functions, and nonsmooth event-triggered control, the proposed approach ensures high tracking accuracy, strict constraint enforcement, and reduced control effort.

Unlike conventional Sliding Mode Control, the AIBET-NSC controller not only guarantees fixed-time convergence and constraint satisfaction but also produces smooth, chatter-free torque signals that remain within realistic actuator limits. The use of the smooth saturation function and the event-triggered update mechanism leads to continuous and hardware-friendly control inputs, making the scheme suitable for real-time robotic implementation. Simulation results on a 2-DOF manipulator demonstrate superior performance in terms of tracking precision, overshoot suppression, robustness to non-Lipschitz uncertainties, and control update efficiency.

The key contribution of this work lies in the systematic integration of fixed-time nonsmooth control, barrier Lyapunov constraint handling, and algebraic integral observation within an event-triggered framework, offering both strong theoretical guarantees and practical implementability.

Future research will focus on experimental validation on physical robotic platforms, extension to higher-degree-of-freedom manipulators, development of adaptive or optimization-based gain-tuning strategies, and application of the AIBET-NSC scheme in networked or resource-constrained control environments with communication delays and limited bandwidth.

References

[1] T. Belvedere, M. Cognetti, G. Oriolo, and P. R. Giordano, "Sensitivity-aware model predictive control for robots with parametric uncertainty", *IEEE Transactions on Robotics*, Vol. 41, pp. 3039-3058, 2025. DOI: 10.1109/TRO.2025.3554415

[2] G. Shen, P. Huang, Z. Ma, F. Zhang, and Y. Xia, "Dynamic event-based adaptive fixed-time control for uncertain strict-feedback nonlinear systems with state constraints", *IEEE Transactions on Cybernetics*, Vol. 54, No. 8, pp. 4630-4642, Aug. 2024. DOI: 10.1109/TCYB.2023.3293466

[3] B. Bandyopadhyay and A. K. Behera, *Event-Triggered Sliding Mode Control*. Springer, 2018. DOI: 10.1007/978-3-319-74219-9

[4] X. Ding *et al.*, "Online control barrier function construction for safety-critical motion control of manipulators", *IEEE Transactions on Systems, Man, and Cybernetics: Systems*, Vol. 54, No. 8, pp. 4761-4771, Aug. 2024. DOI: 10.1109/TSMC.2024.3387434

[5] H. Sai *et al.*, "Chattering-free fast fixed-time sliding mode control for uncertain robotic manipulators", *International Journal of Control, Automation and Systems*, Vol. 21, pp. 630-644, 2023. DOI: 10.1007/s12555-021-0823-4

[6] F. Deng, Q. Wen, and L. Yang, "Model-free sliding mode prescribed performance control of robotic manipulator based on new reaching law", *International Journal of Advanced Robotic Systems*, Vol. 20, No. 4, 2023. DOI: 10.1177/17298806231191002

[7] J. Hu *et al.*, "Finite-time adaptive super-twisting sliding mode control for autonomous robotic manipulators with actuator faults", *ISA Transactions*, Vol. 144, pp. 342-351, 2024. DOI: 10.1016/j.isatra.2023.10.028

[8] C. Jing, H. Zhang, Y. Liu, and J. Zhang, "Adaptive super-twisting sliding mode control for robot manipulators with input saturation", *Sensors*, Vol. 24, No. 9, 2024. DOI: 10.3390/s24092783

[9] Z. Xie, X. Chen, and X. Wu, "Fixed time control of free-flying space robotic manipulator with full state constraints: a barrier-Lyapunov-function term free approach", *Nonlinear Dynamics*, Vol. 112, pp. 1883-1915, 2024. DOI: 10.1007/s11071-023-09097-z

[10] T. Zhang and P. Yan, "Asymmetric integral barrier function-based tracking control of constrained robots", *AIMS Mathematics*, Vol. 9, No. 1, pp. 319-339, 2024. DOI: 10.3934/math.2024019

[11] J. Li, X. Wang, R. Jiao, and M. Dong, "Asymmetric integral barrier lyapunov function-based human-robot interaction control for human-compliant space-constrained muscle strength training", in *IEEE Transactions on Systems, Man, and Cybernetics: Systems*, Vol. 54, No. 7, pp. 4305-4317, July 2024. DOI: 10.1109/TSMC.2024.3378479

[12] T. Wang and Y. Chen, "Event-triggered control of flexible manipulator constraint system modeled by PDE", *Mathematical Biosciences and Engineering*, Vol. 20, No. 6, pp. 10043-10062, 2023. DOI: 10.3934/mbe.2023441

[13] T. Berger, "On observers for nonlinear differential-algebraic systems", in *IEEE Transactions on Automatic Control*, Vol. 64, No. 5, pp. 2150-2157, May 2019. DOI: 10.1109/TAC.2018.2866438

[14] A. Kanel-Belov *et al.*, "Nonstandard analysis, deformation quantization and some logical aspects of (non)commutative algebraic geometry", *Mathematics*, Vol. 8, No. 10, 2020. DOI: 10.3390/math8101694

[15] Z. Liu, X. Cui, Z. Zhao, and K. S. Hong, "PDE-based consensus control for multiagent systems with event-triggered mechanism", in *IEEE Transactions on Control of Network Systems*, Vol. 11, No. 4, pp. 1768-1777, 2024. DOI: 10.1109/TCNS.2024.3355047

[16] G. Wang, W. Yuan, and X. Wang, "Event-triggered adaptive neural network backstepping sliding fault-tolerant control of spacecraft formation flying with input saturation", *International Journal of Aerospace Engineering*, Vol. 2024, 2024. DOI: 10.1155/2024/6847067

[17] T. Li *et al.*, " Event-triggered tracking control for nonlinear systems subject to time-varying external disturbances", *Automatica*, Vol. 119, 2020. DOI: 10.1016/j.automatica.2020.109070.

[18] G. B. Avanzini, A. M. Zanchettin, and P. Rocco, "Constrained model predictive control for mobile robotic manipulators", *Robotica*, Vol. 36, No. 1, pp. 19-38, 2018. DOI: 10.1017/S0263574717000133

[19] X. Jin, Y. X. Li, and S. Tong, "Adaptive event-triggered control design for nonlinear systems with full state constraints", in *IEEE Transactions on Fuzzy Systems*, Vol. 29, No. 12, pp. 3803-3811, 2021. DOI: 10.1109/TFUZZ.2020.3028645

[20] X. M. Zhang *et al.*, "An overview of recent advances in event-triggered control", *Science China Information Sciences*, Vol. 68, Iss. 6, 2025. DOI: 10.1007/s11432-024-4437-9

[21] Z. Li and J. Zhao, "A zeno-free event-triggered control strategy for asymptotic stabilization of switched affine systems", in *IEEE Transactions on Automatic Control*, Vol. 67, No. 10, pp. 5509-5516, 2022. DOI: 10.1109/TAC.2021.3120676

[22] P. Gierlak, "Adaptive position/force control of a robotic manipulator in contact with a flexible and uncertain environment", *Robotics*, Vol. 10, No. 1, 2021. DOI: 10.3390/robotics10010032

[23] A. Hmidet, R. Dhifaoui, and O. Hasnaoui, "A new direct speed estimation and control of the induction machine benchmark: Design and experimental validation", *Mathematical Problems in Engineering*, 2018. DOI: 10.1155/2018/9215459

[24] Z. Dachang *et al.*, "Adaptive nonsingular terminal sliding mode control of robot manipulator based on contour error compensation", *Scientific Reports*, Vol. 13, No. 330, 2023. DOI: 10.1038/s41598-023-27633-0

[25] C. Zhao and W. Lin, "Homogeneity, forward completeness, and global stabilization of a family of time-delay nonlinear systems by memoryless non-lipschitz continuous feedback", in *IEEE Transactions on Automatic Control*, Vol. 67, No. 11, pp. 5916-5931, 2022. DOI: 10.1109/TAC.2021.3124992

[26] M. B. Çetinkaya, K. Yildirim, and Ş. Yildirim, "Trajectory analysis of 6-DOF industrial robot manipulators by using artificial neural networks", *Sensors*, Vol. 24, No. 13, 2024. DOI: 10.3390/s24134416

[27] S. Kariuki *et al.*, "Pick and place control of a 3-DOF robot manipulator based on image and pattern recognition", *Machines*, Vol. 12, No. 9, 2024. DOI: 10.3390/machines12090665

[28] S. Mustary *et al.*, " Advancing stability in robot manipulators: A review of recent progress and parameters", *Engineering Reports*, No. 7, 2025. DOI: 10.1002/eng2.70207

[29] L. Zhang and X. Yao, "Two-layer adaptive composite anti-disturbance control for robotic manipulator with multiple disturbances", in: Yan, L., Duan, H., Deng, Y. (eds) *Advances in Guidance, Navigation and Control. ICGNC 2024*, *Lecture Notes in Electrical Engineering*, Vol. 1353, Springer, 2024. DOI: 10.1007/978-981-96-2264-1_3

[30] A. Polyakov, "Nonlinear feedback design for fixed-time stabilization of linear control systems", in *IEEE Transactions on Automatic Control*, Vol. 57, No. 8, pp. 2106-2110, 2012. DOI: 10.1109/TAC.2011.2179869

[31] J. Zhai, H. Wang, and Z. He, "Fixed-time tracking control for high-order nonlinear systems with unknown time-varying input delay", *Applied Mathematics and Computation*, Vol. 452, 2023. DOI: 10.1016/j.amc.2023.128027

[32] X. Wang and S. Wang, "Fixed-time integral terminal sliding-mode control with super-twisting nonlinear extended-state observer for servo system with disturbances", *IEEE Journal of Emerging and Selected Topics in Industrial Electronics*, Vol. 6, No. 1, pp. 435-446, 2025. DOI: 10.1109/JESTIE.2024.3417375

[33] M. Rahmani, H. Komijani, and M. H. Rahman, "New sliding mode control of 2-DOF robot manipulator based on extended grey wolf optimizer", *International Journal of Control, Automation and Systems*, Vol. 18, pp. 1572-1580, 2020. DOI: 10.1007/s12555-019-0154-x

[34] Z. Song *et al.*, "Adaptive dynamic boundary sliding mode control for robotic manipulators under varying disturbances", *Electronics*, Vol. 13, No. 5, 2024. DOI: 10.3390/electronics13050900

[35] Z. Bingul and K. Gul, "Intelligent-PID with PD feedforward trajectory tracking control of an autonomous underwater vehicle", *Machines*, Vol. 11, No. 2, 2023. DOI: 10.3390/machines11020300

ĐIỀU KHIỂN KHÔNG TRƠN KÍCH HOẠT THEO SỰ KIỆN DỰA TRÊN TÍCH PHÂN ĐẠI SỐ VÀ HÀM LYAPUNOV RÀO CHẮN CHO TAY MÁY RÔ BỐT NHIỀU BẬC TỰ DO DƯỚI TÁC ĐỘNG CỦA NHIỄU KHÔNG LIPSCHITZ

Hoàng Đức Long[1]

[1]*Viện Kỹ thuật điều khiển, Trường Đại học Kỹ thuật Lê Quý Đôn*

Tóm tắt: Bài báo trình bày một cấu trúc điều khiển mới, gọi là điều khiển không trơn kích hoạt theo sự kiện dựa trên tích phân đại số và hàm Lyapunov rào chắn (AIBET-NSC), nhằm điều khiển bám quỹ đạo một cách bền vững cho các tay máy rô bốt nhiều bậc tự do trong điều kiện có nhiễu không Lipschitz. Phương pháp đề xuất tích hợp bốn thành phần chính: (i) bộ quan sát tích phân đại số giúp ước lượng trạng thái bền vững trước nhiễu đo; (ii) hàm Lyapunov rào chắn (BLF) để đảm bảo chặt chẽ giới hạn của các biến khớp; (iii) luật điều khiển không trơn dựa trên điều khiển trượt nhằm đảm bảo hội tụ sai số trong thời gian hữu hạn; và (iv) cơ chế kích hoạt theo sự kiện giúp giảm đáng kể tần suất cập nhật điều khiển mà không làm mất ổn định hệ thống. Khác với phương pháp điều khiển trượt cổ điển (SMC), AIBET-NSC đảm bảo hội tụ trong thời gian cố định từ bất kỳ điều kiện ban đầu nào, đồng thời giảm thiểu hiện tượng dao động và khối lượng tính toán. Phân tích lý thuyết đã chứng minh tính ổn định toàn cục trong thời gian cố định và cơ chế kích hoạt không xảy ra hiện tượng Zeno dưới tác động của các nhiễu bị chặn. Kết quả mô phỏng cho thấy AIBET-NSC vượt trội so với SMC truyền thống bao gồm thời gian ổn định nhanh hơn, độ quá điều chỉnh nhỏ hơn, mô men điều khiển mượt hơn và số lần cập nhật ít hơn.

Từ khóa: *Điều khiển kích hoạt theo sự kiện; hàm Lyapunov rào chắn; ổn định trong thời gian cố định; điều khiển không trơn; nhiễu không Lipschitz; cánh tay rô bốt.*

Received: 17/09/2025; Revised: 28/10/2025; Accepted for publication: 27/01/2026

❑